Turbulence intensity measurement in the wind tunnel used for airfoil flutter investigation

Petr Šidlof[1,a] , *Pavel* Antoš[2], *David* Šimurda[2], *Martin* Štěpán[1]

[1]Technical University of Liberec, NTI FM, Studentská 2, 461 17 Liberec 1, Czech Republic
[2]Institute of Thermomechanics, Academy of Sciences of the Czech Republic, Dolejškova 5, 182 00 Prague 8, Czech Republic

Abstract. The paper reports on hot wire turbulence intensity measurements performed in the entry of a suction-type wind tunnel, used for investigation of flow-induced vibration of airfoils and slender structures. The airfoil is elastically supported with two degrees of freedom (pitch and plunge) in the test section of the wind tunnel with lateral optical access for interferometric measurements, and free to oscillate. The turbulence intensity was measured for velocities up to M = 0.3 i) with the airfoil blocked, ii) with the airfoil self-oscillating. Measurements were performed for a free inlet and further with two different turbulence grids generating increased turbulence intensity levels. For the free inlet and static airfoil, the turbulence intensity lies below 0.4%. The turbulence grids G1 and G2 increase the turbulence level up to 1.8% and 2.6%, respectively. When the airfoil is free to oscillate due to fluid-structure interaction, its motion disturbs the surrounding flow field and increases the measured turbulence intensity levels up to 5%.

1 Introduction

The aircraft lifting surfaces (wings, flaps and ailerions, stabilators, elevons and rudders), helicopter blades, propellers, turbine or compressor blades are slender structures subjected to unsteady aerodynamic forces and moments. As such, they are potentially susceptible to aeroelastic instability such as coupled-mode flutter, stall flutter or dynamic stall. A comprehensive review on flutter and dynamic stall is given in [1], a practical guide for technical designers can be found in [2]. Fluid-structure interaction can lead to catastrophic consequences, and thus the aircraft components must be carefully designed and tested in order to ensure that the aeroelastic instability never occurs within the operating conditions.

During last years, the fundamental properties of a self-oscillating NACA0015 airfoil with two degrees of freedom have been studied in a high-speed suction-type wind tunnel of the Institute of Thermomechanics in Nový Knín [3]. For low inlet air speeds, damped oscillations were observed. When the elastically supported airfoil is subjected to flow of higher velocity, the system becomes aeroelastically unstable and any motion of the airfoil induced by an initial impulse or disturbance in the flow exponentially increases. Due to nonlinearity of the system, the oscillations finally stabilize in limit cycle oscillations (LCO) of certain frequency and amplitude, strongly dependent on the mechanical properties of the system (stiffness of the springs, mass distribution, mechanical damping, eigenfrequencies of the pitching and plunging modes). The experimental setup allows dynamic measurement of the flow-induced oscillations and time-resolved measurements of the static pressure at four pressure ports on the surface of the airfoil. Synchronously, the flow fields around the airfoil can be monitored either using time-resolved interferometric measurements [3,4] or Schlieren visualizations [5].

The test section is located shortly downstream of the free entry of the wind tunnel. In this configuration, the turbulence intensity of the flow should be quite low. The purpose of the current study is to measure the turbulence intensity levels when different turbulence grids are fixed upstream of the test section, and compare them to the case when no turbulence grid is present.

2 Experimental setup

The model design builds on previous experience obtained in the Institute of Thermomechanics in the years 2006-2012, when self-oscillating models of the NACA0015 and DCA18% airfoils with two degrees of freedom were designed and the methodology of the measurements developed [6,7,3]. The airfoil, supported by a linear and torsional springs, is fixed in a suction-type wind tunnel with optical access through the side walls for Schlieren visualizations and interferometric measurements of the flow field.

2.1 Mechanical setup

The NACA0015 airfoil is supported by vertical guides, freely moving in the vertical direction, and rotating around the elastic axis in 1/3 of the chord length (see Fig. 1 and 2).

* Corresponding author: petr.sidlof@tul.cz

Fig. 1. Model of the pitch-plunge airfoil in the wind tunnel (side view).

The test section has a cross-section of 80 x 210 mm, with the free opening of the wind tunnel 310 mm upstream of the airfoil leading edge.

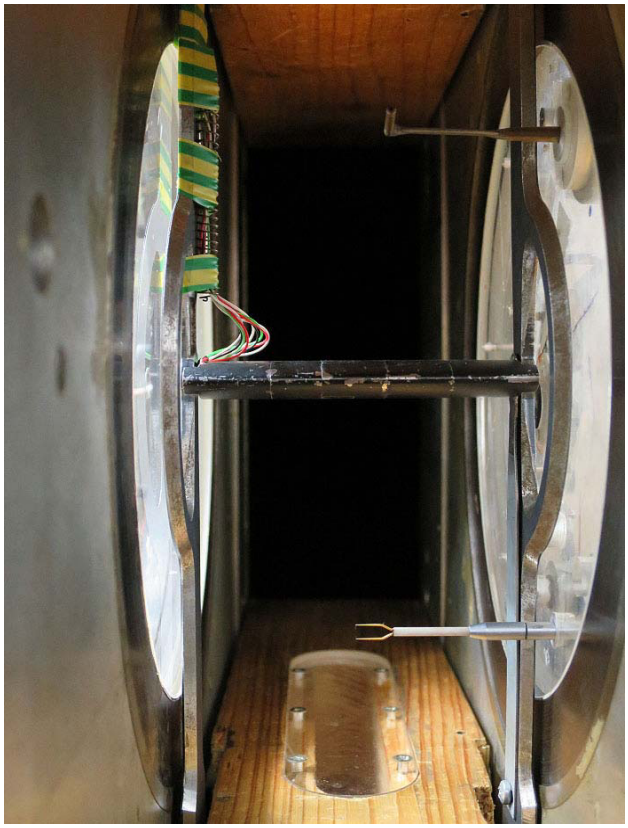

Fig. 2. Airfoil and hot-wire probe (view from inlet part of wind tunnel).

The airfoil has a chord length of 59.5 mm, considerable smaller than comparable self-oscillating airfoil designs, e.g. [8-13]. The stiffness of the flat springs is 16 383 N/m, resulting in the still-air natural frequency of the plunging mode f_{plunge} = 14.6 Hz. In current configuration, the eigenfrequency of the torsional mode is f_{pitch} = 17.8 Hz.

2.2 Motion and pressure sensors

Due to the size of the airfoil (chord 59.5 mm, maximum thickness 9 mm), there is a very limited space for installation of the sensors inside the model. The airfoil is equipped with a miniature rotary magnetic encoder (RLS - Renishaw RM08) measuring the pitch angle, and four dynamic piezoresistive pressure sensors with built-in preamplifiers (Freescale Semiconductor MPXH6115) mounted flush with the airfoil surface. The pressure sensors are denoted p_{1U}, p_{2U} (upper surface) and p_{1L}, p_{2L} (lower surface) and are located 10.8 mm and 29.5 mm from the leading edge, respectively (see Fig. 3).

Outside of the test section, the vertical deflection of the airfoil is measured by a laser triangulation sensor (MicroEpsilon optoNCDT ILD-2200). An additional strain gauge bridge is mounted on the flat spring supporting the airfoil frame and calibrated to provide a redundant signal of the deflection.

The signals from the airfoil pressure transducers, strain gauge bridge and the triangulation sensor are digitized, monitored online and stored by a Dewetron data acquisition system. The software includes a special module for triggering of the high-speed camera, which enables perfect synchronization of the recorded interferograms with the signals from all the sensors.

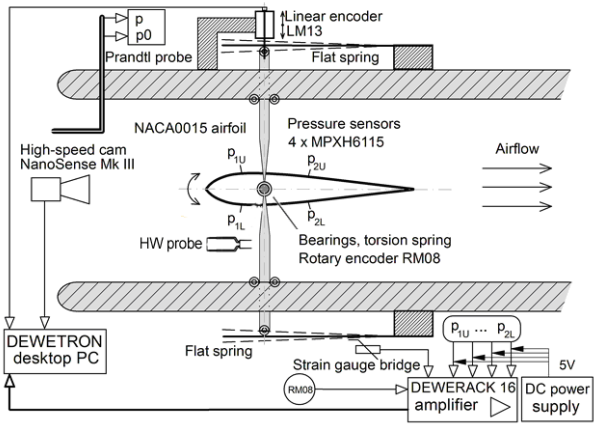

Fig. 3. Mechanical sensors, HW probe and electrical connections

2.3 Optical measurements

The test section of the wind tunnel and its special lateral optical glasses are designed for measurements of the flow field using the Mach-Zehnder interferometer and for Schlieren visualizations. The former method, used within current study, is sensitive to the air density which has local variations due to compressibility effects, the latter to the density gradient [14]. More details regarding the optical configuration can be found in [5].

2.4 Grid generators

Two grid turbulence generators denoted as G1 and G2 were tested during the measurements (see Fig. 4). The grids are manufactured from an interwoven steel wire, and are fixed 140mm downstream of the wind tunnel

entry. The parameters of the grids are summarized in Tab. 1.

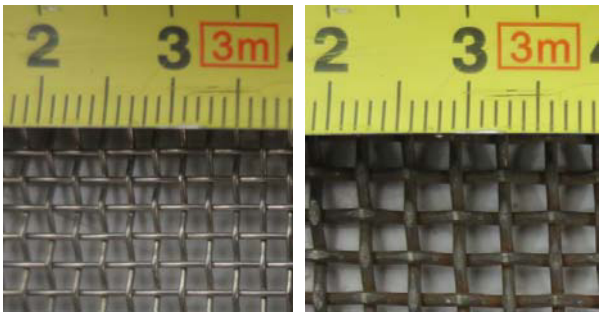

Figure 4. Grids G1 (left) and G2 (right)

Table 1. Wire diameter, grid spacing and mesh size.

	diam [mm]	spacing [mm]	mesh size [mm]
G1	0.5	1.6	2.1
G2	0.95	2.0 (vertically) 2.4 (horizontally)	2.95 (vertically) 3.4 (horizontally)

2.5 Hot-wire measurements

The hot-wire probe was placed 260 mm downstream of the wind tunnel entry. It was in the plane of the leading edge of the airfoil, i.e. 120 mm downstream of the turbulence grid.

A single-sensor probe DANTEC 55P01 was used for the measurement in flow. The sensor is a tungsten wire with gold-plated ends of the diameter d_w=5 μm and the active length l_w=1.25 mm. The probe was calibrated in the rig with variable flow velocity in the range of velocities U=(2-140) m/s. Sensor was operated at CTA mode with wire temperature T_w=513 K. Details about principle of HWA measurement and its evaluation can be found in [15].

The CTA system DANTEC Streamline was used. The output signals are then digitalized using the A/D transducer (National Instruments data acquisition system 16 bit) with sampling frequency 250 kHz.

3 Results

The turbulence intensity measurements were performed for a set of inlet flow velocities ranging from Ma = 0.1 to Ma = 0.3. Three cases were tested: without turbulence grid, and with grids G1 and G2 mounted. In most cases, the airfoil motion was blocked to measure the turbulence intensity in the flow field undisturbed by airfoil oscillations, but three cases were also tested when the airfoil was free and under flow-induced vibration with quite large amplitudes (up to 8.3 mm in vertical motion and 27.6 deg in rotation).

The results of mechanical and optical measurements are reported and summarized in Tab. 2.

Table 2. Measurement by mechanical sensors. Used grid generator of turbulence, inlet flow Mach number, status of the airfoil support. Frequency of flow-induced vibration, amplitude of the plunging and pitching mode.

No.	Ident.	grid	Ma [-]	airfoil	$f_{airfoil}$ [Hz]	A_y [mm]	A_φ [deg]
5	2958-5	-	0.1	blocked	-	-	-
6	2958-6	-	0.15	blocked	-	-	-
7	2958-7	-	0.15	free	-	-	-
8	2958-8	-	0.2	blocked	-	-	-
9	2958-9	-	0.2	free	17.5	2.5	29.5
10	2958-10	-	0.25	blocked	-	-	-
11	2958-11	-	0.25	free	17.5	4.1	28.9
12	2958-12	-	0.3	blocked	-	-	-
13	2958-13	-	0.3	free	16.7	8.3	27.6
14	2958-14	G1	0.1	blocked	-	-	-
15	2958-15	G1	0.15	blocked	-	-	-
16	2958-16	G1	0.2	blocked	-	-	-
17	2958-17	G1	0.25	blocked	-	-	-
18	2958-18	G1	0.3	blocked	-	-	-
19	2958-19	G2	0.1	blocked	-	-	-
20	2958-20	G2	0.15	blocked	-	-	-
21	2958-21	G2	0.2	blocked	-	-	-
22	2958-22	G2	0.25	blocked	-	-	-
23	2958-23	G2	0.3	blocked	-	-	-

The graph of velocity U and turbulence intensity I_u during measurements No. 5, 6, 8, 10, 12 is given in Figure 5. This is the case of flow without grid generator with blocked airfoil.

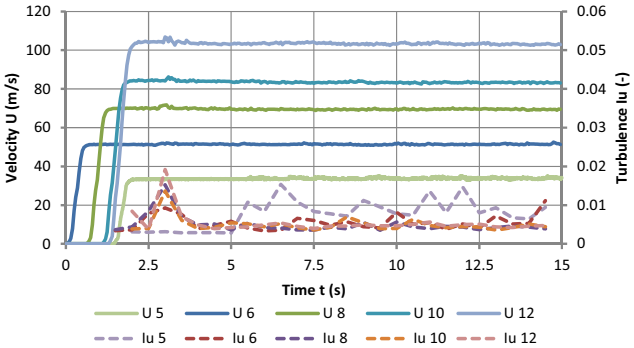

Fig. 5. Measurements No. 5, 6, 8, 10, 12 with blocked airfoil and no grid generator.

The plot in Fig. 6 shows measurements No. 7, 9, 11, 13 with free airfoil. The oscillations in flow field induced by the airfoil motion are clearly visible. For computation of turbulence intensity, the hot-wire signal was processed by high-pass filter at 500 Hz to extract amplitudes from low frequencies.

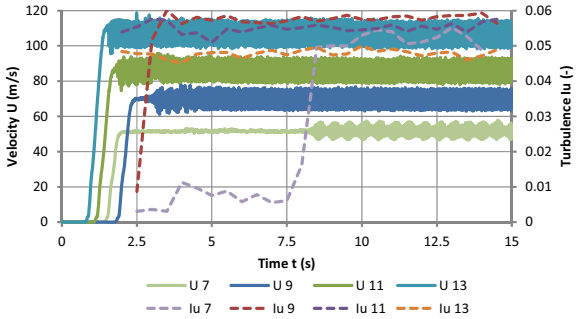

Fi. 6. Measurements No. 7, 9, 11, 13 with free airfoil and no grid generator.

Next two graphs in Fig. 7 and 8 show measurements No. 14-22 with blocked airfoil and grid generators of turbulence G1 and G2.

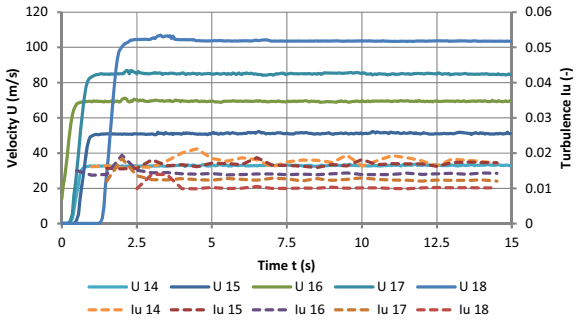

Fig. 7. Measurements No.14-18 with blocked airfoil and grid generator G1.

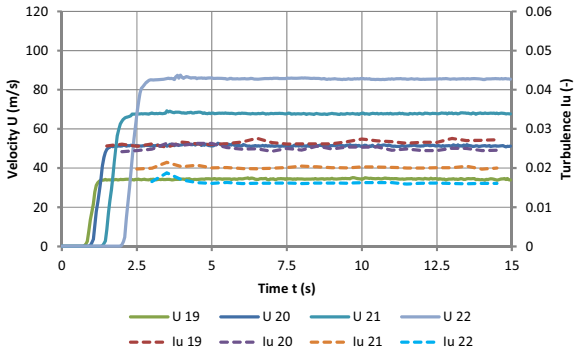

Fig. 8. Measurements No. 19-22 with blocked airfoil and grid generator G2.

Spectra of flow velocity fluctuations from the HW signal are shown below. The FFT spectrum in case of blocked airfoil and grid G1 is shown in Fig. 9.

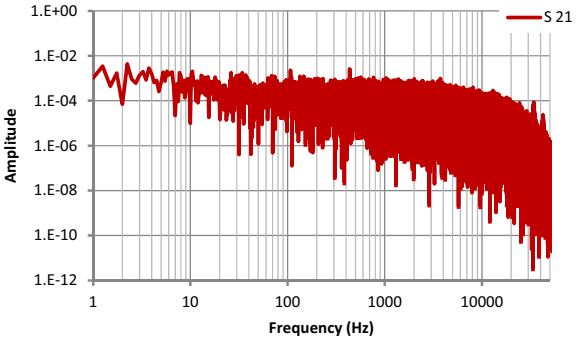

Fi. 9. Spectrum of the HW signal in measurement No. 21. Blocked airfoil, grid G2.

Spectra of flow with free airfoils are plotted for measurements No. 7, 9, 11 and 13. The spectrum of measurement No. 7 in Fig. 10 shows significant peaks at frequencies 15.750 Hz (100%A); 17.746 Hz (38%A); 13.783 Hz (9%A); 19.711 Hz (2%A). In this case, the airfoil is free, but the flow velocity is not sufficient to trigger the aeroelastic instability. In all other measurements (with higher velocities) a single dominant frequency is seen, matching perfectly the frequency of airfoil oscillation obtained from mechanical sensor measurements.

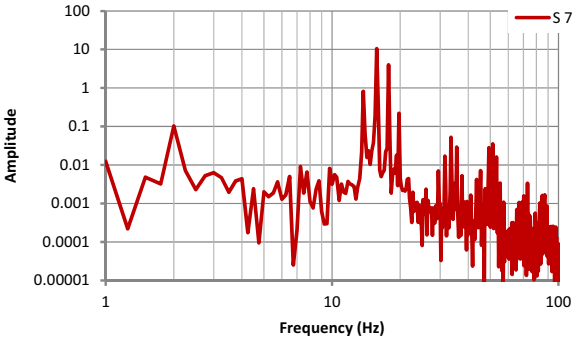

Fig. 10. Spectrum from measurement No. 7. Free airfoil, no airfoil oscillation.

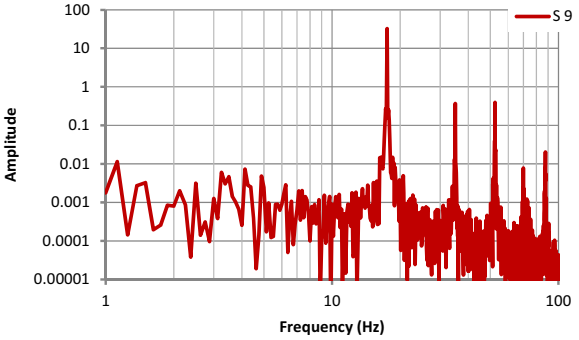

Fig. 11. Spectrum from measurement No. 9. Free airfoil, limit cycle oscillations at 17.49 Hz.

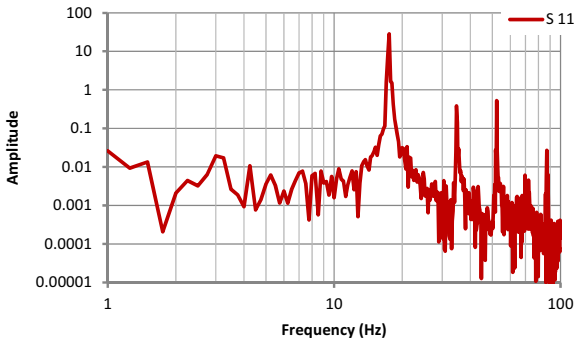

Fig. 12. Spectrum from measurement No. 11. Free airfoil, limit cycle oscillations at 17.47 Hz.

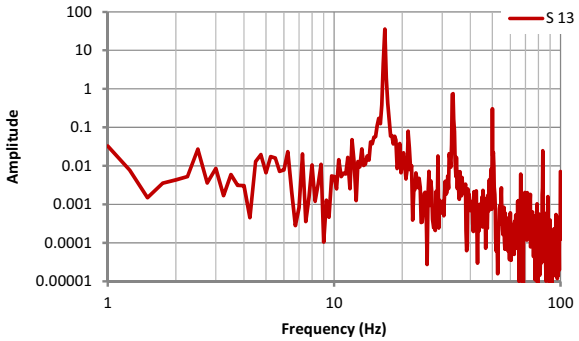

Fig. 13. Spectrum from measurement No. 13. Free airfoil, limit cycle oscillations at 16.73 Hz.

The results of the turbulence intensity measurements are summarized in Table 3.

Table 3. HWA measured data. Mean velocity, turbulence intensity level and frequency of peak in spectrum of the flow around the airfoil.

No.	grid	Ma [-]	airfoil	I_u [%]	f_{flow} [Hz]
5	-	0.1	blocked	0.28*	-
6	-	0.15	blocked	0.33*	-
7	-	0.15	free	5.2	15.750
8	-	0.2	blocked	0.35*	-
9	-	0.2	free	5.78	17.499
10	-	0.25	blocked	0.35*	-
11	-	0.25	free	5.5	17.471
12	-	0.3	blocked	0.37*	-
13	-	0.3	free	4.78	16.736
14	G1	0.1	blocked	1.79	-
15	G1	0.15	blocked	1.68	-
16	G1	0.2	blocked	1.41	-
17	G1	0.25	blocked	1.25	-
18	G1	0.3	blocked	1.01	-
19	G2	0.1	blocked	2.65	-
20	G2	0.15	blocked	2.51	-
21	G2	0.2	blocked	2.02	-
22	G2	0.25	blocked	1.62	-
23	G2	0.3	blocked	-	-

* Minimal value of Iu

4 Discussion and conclusions

The turbulence intensity levels in the entry of the wind tunnel test section used for investigation of the aeroelastic instability of an airfoil with two degrees of freedom were investigated. In case of blocked airfoil, when the inlet part of the wind tunnel is free, the turbulence level at the airfoil leading edge ranges from 0.28% to 0.37%. When the fine turbulence grid G1 is mounted, the turbulence intensity is 1.79% for the lowest flow speed Ma = 0.1 and 1.01% for the highest possible flow speed Ma = 0.3. The coarse turbulence grid G2 induces turbulence levels ranging from 2.65% to 1.62%, decreasing with increasing flow velocity.

In the case of self-oscillating airfoil, the motion heavily disturbs the surrounding flow field and the measured intensity of turbulence were of levels of 4.78% - 5.78%.

In spectra of flow obtained from HW measurements were found significant peaks at frequencies of 15.750 Hz, 17.499 Hz, 17.471 Hz, 16.736 Hz, which match the frequencies of airfoil oscillation from mechanical measurements (N/A, 17.5 Hz, 17.5 Hz, 16.7 Hz).

Acknowledgements

The research has been supported by the Czech Science Foundation, project 13-10527S "Subsonic flutter analysis of elastically supported airfoils using interferometry and CFD". The experimental data were acquired during measurements in the wind tunnel of the Institute of Thermomechanics, Academy of Sciences of the Czech Republic in Nový Knín, in cooperation with Martin Luxa, Jaromír Horáček and Václav Vlček.

References

1. W. J. McCroskey, Annual Review Of Fluid Mechanics **14**, 1 (1982)
2. L. Ericsson, J. Reding, Journal of Fluids and Structures **2,** 1 (1988)
3. P. Šidlof, V. Vlček, M. Štěpán, J. Horáček, M. Luxa, D. Šimurda, J. Kozánek, *Proceedings of the ASME PVP 2014 conference* (ASME, 2014)
4. P. Šidlof, Š. Riss, V. Vlček V., *Topical Problems of Fluid Mechanics* (2016),
5. P. Šidlof, V. Vlček, M. Štěpán, Journal of Fluids and Structures (2016, in press)
6. V. Vlček, J. Kozánek, Acta Technica **56** (2011)
7. J. Kozánek, V. Vlček, I. Zolotarev I., International Journal of Structural Stability and Dynamics **13,** 7 (2013)
8. T. O'Neil, T. W. Strganac T. W., Journal of Aircraft **35,** 4 (1998)
9. C. Marsden, S. Price S, Journal of Fluids and Structures **21,** 3 (2005)
10. E. Tinar, O. Cetiner, Experiments in Fluids **41,** 2 (2006)
11. D. Poirel, Y. Harris, A. Benaissa, Journal of Fluids and Structures **24,** (2008)

12. M. Schwartz. S. Manzoor, P. Hémon, E. de Langre., Journal of Fluids and Structures **25**, 8 (2009)
13. N. A. Razak, T. Andrianne, G. Dimitriadis, AIAA Journal **49**, 10 (2011)
14. A. H. Shapiro, *The Dynamics and Thermodynamics of Compressible Fluid Flow* (The Ronald Press Company, 1954)
15. P. Antoš, EPJ Web of Conferences **25**, 01004 (2012)